

Design Of Compact E-Shape Microstrip Patch Antenna For 4G Communication Systems

Hari Shankar Tiwari,
PG Scholar,
Department of Electronics &
Communication Engg., RITS,
Bhopal

Manoj Singh Rawat,
PG Scholar,
Department of Electronics &
Communication Engg., BUIT,
Bhopal

Prof. Amit Rajput
Professor,
Department of Electronics &
Communication Engg., RITS,
Bhopal

Abstract

In this paper, the design and analysis of E-shape microstrip patch antenna for the 4G mobile communication system is presented. The shape of proposed antenna will provide the wide bandwidth which is required for the operation of 4G mobile communication systems. The operating frequency of antenna is 3GHz, The antenna design consists of a single layer of thickness 1.6 mm with dielectric constant of 4.2 and fabricated on glass epoxy material. The simulation results of proposed E-Shape antenna are done by the help of IE3D Zeland Software (Version 12.0). For the analysis of antenna we used the Cavity Model. This antenna is fed by a co-axial probe feeding. The effects of different antenna parameters like return loss, voltage standing wave ratio (VSWR) are also studied.

Keywords— Microstrip patch antenna, Return loss, VSWR.

1. Introduction

As the developments has been done for improvement of wireless communications, the necessity to design low volume, compact, low profile planar configuration and wideband multi-frequency planar antennas become extremely popular. Narrow bandwidth is a serious restriction of these microstrip patch antennas. Different kinds of techniques are used to overcome this narrow bandwidth restriction. These techniques comprise using parasitic patches [1], increasing the thickness of the dielectric substrate and decreasing dielectric constant [2].

The approach of the microstrip antenna enjoys all the advantages of printed circuit technology. The other drawbacks of basic microstrip structures include low power handling capability, loss, half plane radiation and limitation on the maximum gain. For many practical

designs, the advantages of microstrip antennas far compensate their disadvantages [2]. However, research is still ongoing today to conquer some of these disadvantages. This paper, introduces designing and an analysis of E-shape microstrip patch antenna for 4G Mobile communication applications. The E-shape of microstrip patch antenna as shown in Figure 1.

2. Antenna Design and Structure

A. E-Shaped Microstrip Antenna

The proposed configuration of the antenna is shown in Figure 1. The antenna design consists of a single layer of thickness 1.6 mm. The dielectric constant of the substrate is 4.2 and antenna is fabricated on glass epoxy material. The E-shaped antenna is formed by inserting [19] the coordinate or by removing the inserted points from the rectangular patch of suitable dimension. Two parallel slots are incorporated inside the rectangular patch antenna to perturb the surface current path. The probe is feed at point (27, 2.5) as shown in Figure 1.

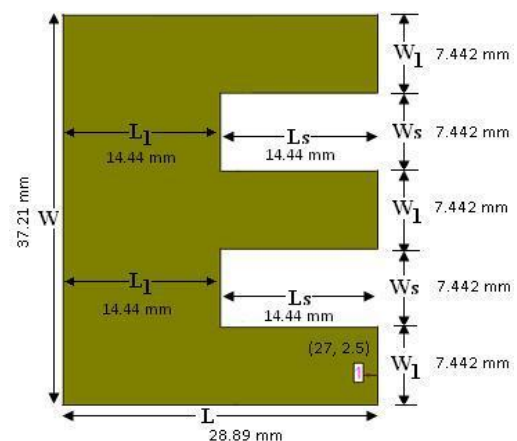


Figure 1. Probe fed E-Shape microstrip antenna with dimensions

The E-shaped is simpler in construction. The two parallel slots have the same length L_s and the same width W_s . The separation [15, 12] of the two slots is W_1 . There are thus only three parameters (L_s , W_s , W_1) for the slots used here. A probe feed a point (27, 2.5) located for good excitation of the proposed antenna over a wide bandwidth.

B. Design Equation

Because of the fringing effects, electrically the patch of the antenna looks larger than its physical dimensions the enlargement on L is given by:

$$\Delta L = \frac{0.412h(\epsilon_{reff} + 0.3)(Wh^{-1} + 0.264)}{[(\epsilon_{reff} - 0.258)(Wh^{-1} + 0.8)]} \quad (2.1)$$

Where the effective (relative) permittivity is,

$$\epsilon_{reff} = \frac{\epsilon_r + 1}{2} + \frac{\epsilon_r - 1}{2\sqrt{1 + 12hW^{-1}}} \quad (2.2)$$

This is related to the ratio of h/W. The larger the h/W, the smaller the effective permittivity [1,7]. The effective length of the patch is given by:

$$L_{eff} = L + 2\Delta L \quad (2.3)$$

The resonant frequency for the TM_{100} mode is:

$$f_r = 1/\left[2L_{eff}\sqrt{\epsilon_{reff}\sqrt{\epsilon_0\mu_0}}\right] \quad (2.4)$$

$$f_r = 1/\left[2(L + 2\Delta L)\sqrt{\epsilon_{reff}\sqrt{\epsilon_0\mu_0}}\right] \quad (2.5)$$

An optimized width for an efficient radiator is,

$$W = 1/(2f_r\sqrt{\epsilon_0\mu_0}) \times \sqrt{2/\epsilon_r + 1} \quad (2.6)$$

C. Design Procedure

If the substrate parameter (ϵ_r and h) and the operating frequency (f_r) are known than we can easily calculate the dimensions of the patch antenna using above simplified equation following design procedure to design the antenna:

Step 1: Using equation (2.6) to find out the patch width W.

Step 2: Calculate the effective permittivity using the equation (2.2)

Step 3: Compute the extension of the length using the equation (2.1)

Step 4: Determine the length L by solving the equation for L giving the solution.

$$L = [1/(2f_r\sqrt{\epsilon_{reff}\sqrt{\epsilon_0\mu_0}})] - 2\Delta L \quad (2.7)$$

Table 1. Dimensions of the Prescribed Antenna

Frequency	3GHz
W	37.21 mm
W_1	7.442 mm
W_s	7.442 mm
L	28.89 mm
L_1	14.44 mm
L_s	14.44 mm
Dielectric (ϵ_r)	4.2
Thickness (h)	1.6mm

3. Method of Analysis

There are many methods of analysis for microstrip antennas. The microstrip antenna generally has a two-dimensional radiating patch on a thin dielectric substrate and therefore may be categorized as a two-dimensional planar component for analysis purposes. The analysis methods for microstrip antennas can be broadly divided into two groups. In the first group the methods are based on equivalent magnetic current distribution around the patch edges (similar to slot antennas).

There are three popular analytical techniques [3],

- The Transmission Line Model
- The Cavity Model
- The Multiport Network Model

In the second group, the methods are based on the electric current distribution on the patch conductor and the ground plane (similar to dipole antennas used in conjunction with Full-wave Simulation/Numerical analysis methods). Some of the numerical methods for analyzing microstrip antennas are listed as follows:

- The Method of Moments
- The Finite-Element METHOD
- The Spectral Domain Technique
- The Finite-Difference Time Domain Method

In this work we used the Cavity Model Method.

4. Analysis of E-Shaped Patched Antenna Using Cavity Model

There are many methods of analysis for microstrip antennas. The microstrip antenna analysis either based on equivalent magnetic current distribution around the patch edges (similar to slot antennas) like Cavity Model, Transmission Line Model and Multiport Network Model or based on the electric current distribution on the patch conductor and the ground plane (similar to dipole antennas used in conjunction with full-wave simulation/numerical analysis methods) like FDTD, FEM and Spectral domain technique. In this work we used the cavity model method.

In the cavity model, the region between the patch and the ground plane is treated as a cavity that is surrounded by magnetic walls around the periphery and by electric walls from the top and bottom sides [1]. Since thin substrates are used the field inside the cavity is uniform along the thickness of the substrate. The fringing fields around the periphery are taken care of by extending the patch boundary outward so, that the effective dimensions are larger than the physical dimensions of the patch.

The effect of the radiation from the antenna and the conductor loss are accounted for by adding these losses to the loss tangent of the dielectric substrate. The far field and radiated power are computed from the equivalent magnetic current around the periphery. An alternate way of incorporating the radiation effect in the cavity model is by introducing an impedance boundary condition at the walls of the cavity. Microstrip antennas resemble dielectric loaded cavities and they exhibit higher order resonances. The normalized fields within the dielectric substrate (between the patch and the ground plane) can be found more accurately [10] by treating that region as a cavity bounded by electric conductors (above and below it) and by magnetic walls (to simulate an open circuit) along the perimeter of the patch.

Since the height of the substrate is very small ($h \ll \lambda$) the fields variations along the height will be considered constant. In addition because of the very small substrate height, the fringing of the fields along the edges of the patch is also very small whereby the electric fields is nearly normal to the surface of the patch. Therefore only TM_x field configurations will be considered within the cavity. While the top and bottom walls of the cavity are perfectly electric conducting, the four side walls will be modelled as perfectly conducting magnetic walls (tangential magnetic fields vanish along those four walls).

The linear & inhomogeneous partial differential equation in three dimensions is given by,

$$\nabla^2 A_x + \beta^2 A_x = 0$$

$$\frac{\delta^2}{\delta x^2} A_x + \frac{\delta^2}{\delta y^2} A_y + \frac{\delta^2}{\delta z^2} A_z + \beta^2 A_x = 0 \quad (4.1)$$

Using the method of separation of variable. The solution is assumed in the form of,

$$A_x = X(x)Y(y)Z(z) \quad (4.2)$$

where,

$X(x)$ a function of x only

$Y(y)$ a function of y only

$Z(z)$ a function of z only

Using (1) & (2)

$$YZ \frac{\delta^2}{\delta x^2} X + XZ \frac{\delta^2}{\delta y^2} Y + XY \frac{\delta^2}{\delta z^2} Z + \beta^2 XYZ = 0 \quad (4.3)$$

Dividing (3) by XYZ

$$\frac{1}{X} \frac{\delta^2 X}{\delta x^2} + \frac{1}{Y} \frac{\delta^2 Y}{\delta y^2} + \frac{1}{Z} \frac{\delta^2 Z}{\delta z^2} + \beta^2 = 0 \quad (4.4)$$

$$\frac{1}{X} \frac{\delta^2 X}{\delta x^2} + \frac{1}{Y} \frac{\delta^2 Y}{\delta y^2} + \frac{1}{Z} \frac{\delta^2 Z}{\delta z^2} = -\beta^2 \quad (4.5)$$

The sum of the three terms on the left hand side is a constant and each term is independently variable, it follows that each term must be equal to a constant. Let the three terms are k_x^2 , k_y^2 & k_z^2 then,

$$k_x^2 + k_y^2 + k_z^2 = k^2 \quad (4.6)$$

The general solution of each differential term of the equation (4.5),

$$\frac{1}{X} \frac{\delta^2 X}{\delta x^2} = -k_x^2 \Rightarrow \frac{\delta^2 X}{\delta x^2} = -k_x^2 X \quad (4.7)$$

Similarly,

$$\frac{\delta^2 Y}{\delta y^2} = -k_y^2 Y \quad (4.8)$$

$$\frac{\delta^2 Z}{\delta z^2} = -k_z^2 Z \quad (4.9)$$

will be in form of

$$X = M_1 e^{-jk_x x} + N_1 e^{+jk_x x}$$

$$X = M_1 \cos(k_x x) - jM_1 \sin(k_x x) + N_1 \cos(k_x x) + N_1 \sin(k_x x)$$

$$X = (M_1 + N_1) \cos(k_x x) + j(N_1 - M_1) \sin(k_x x)$$

$$X = A_1 \cos(k_x x) + B_1 \sin(k_x x) \quad (4.10)$$

Similarly,

$$Y = A_2 \cos(k_y y) + B_2 \sin(k_y y) \quad (4.11)$$

$$Z = A_3 \cos(k_z z) + B_3 \sin(k_z z) \quad (4.12)$$

Putting (9) to (11) in (2)

$$A_x = [A_1 \cos(k_x x) + B_1 \sin(k_x x)][A_2 \cos(k_y y) + B_2 \sin(k_y y)][A_3 \cos(k_z z) + B_3 \sin(k_z z)] \quad (4.13)$$

The boundary conditions for 1st rectangle shown in Figure 3, which is cut from Figure 2 are,

$$E_y(x' = 0, 0 \leq y' \leq L_1, 0 \leq z' \leq W) \\ = E_y(x' = h, 0 \leq y' \leq L_1, 0 \leq z' \leq W) \quad (4.14)$$

$$H_y(0 \leq x' \leq h, 0 \leq y' \leq L_1, z' = 0) \\ = H_y(0 \leq x' \leq h, 0 \leq y' \leq L_1, z' = W) \quad (4.15)$$

$$H_z(0 \leq x' \leq h, y' = 0, 0 \leq z' \leq W) \\ = H_z(0 \leq x' \leq h, y' = L_1, 0 \leq z' \leq W) \quad (4.16)$$

x' , y' , z' are the prime numbers and these are used to represent the fields within the cavity.

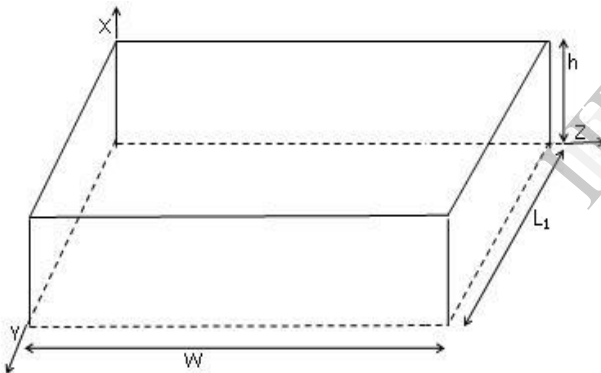


Figure 2. First rectangle

From the boundary conditions (4.14), $B_1 = 0$

$$k_x = m\pi/h, m = 0, 1, 2 \quad (4.17)$$

From (4.16), $B_2 = 0$

$$k_y = n\pi/L_1, n = 0, 1, 2 \quad (4.18)$$

From (4.17), $B_3 = 0$

$$k_z = p\pi/W, p = 0, 1, 2 \quad (4.19)$$

Substitute the value of $B_1 = 0$, $B_2 = 0$ and $B_3 = 0$ in (4.13)

$$A_x = A_1 \cos(k_x x) A_2 \cos(k_y y) A_3 \cos(k_z z) \\ A_x = A_1 A_2 A_3 \cos(k_x x') \cos(k_y y') \cos(k_z z') \quad (4.20)$$

where, $A_{mnp} = A_1, A_2, A_3 =$ amplitude coefficient of each mnp mode

$$A_x = A_{mnp} \cos(k_x x') \cos(k_y y') \cos(k_z z') \quad (4.21)$$

Using (16),(17) & (18)

$$k_x^2 + k_y^2 + k_z^2 = \left(\frac{m\pi}{h}\right)^2 + \left(\frac{n\pi}{L_1}\right)^2 + \left(\frac{p\pi}{W}\right)^2 \\ = k_e^2 = \omega_r^2 \mu \epsilon \quad (4.22)$$

So the resonant frequency for the cavity is given by,

$$(f_r)_{mnp} = \frac{1}{2\pi\sqrt{\mu\epsilon}} \sqrt{\left(\frac{m\pi}{h}\right)^2 + \left(\frac{n\pi}{L_1}\right)^2 + \left(\frac{p\pi}{W}\right)^2} \quad (4.23)$$

$$E_x = -j \frac{1}{\omega\mu\epsilon} [(k^2 - k_x^2) A_{mnp} \\ \cos(k_x x') \cos(k_y y') \cos(k_z z')] \quad (4.24)$$

$$E_y = -j \frac{1}{\omega\mu\epsilon} k_x k_y A_{mnp} \\ \sin(k_x x') \sin(k_y y') \sin(k_z z') \quad (4.25)$$

$$E_z = -j \frac{k_x k_z}{\omega\mu\epsilon} A_{mnp} \\ \sin(k_x x') \cos(k_y y') \sin(k_z z') \quad (4.26)$$

$$H_x = 0 \quad (4.27)$$

$$H_y = -\frac{k_z}{\mu} A_{mnp} \\ \cos(k_x x') \cos(k_y y') \sin(k_z z') \quad (4.28)$$

$$H_z = -\frac{k_y}{\mu} A_{mnp} \\ \cos(k_x x') \sin(k_y y') \cos(k_z z') \quad (4.29)$$

From 1st rectangle, $W = 37.21$ mm & $L_1 = 14.445$ mm. So, $W > L_1 > h$ then the dominant mode is TM_{001}^x .

The value of the k_x, k_y, k_z from (4.17), (4.18) & (4.19),

Using $m = 0, n = 0, p = 1$

$$k_x = m\pi/h = 0 \quad (4.30)$$

$$k_y = n\pi/L_1 = 0 \quad (4.31)$$

$$k_z = p\pi/W = \pi/W \quad (4.32)$$

On putting the value of k_x, k_y, k_z in (4.24), (4.25), (4.26), (4.27), (4.28) & (4.29), we have the resultant fields,

$$E_x = E_0 \cos\left(\frac{\pi}{W} z'\right) \quad (4.33)$$

$$E_y = 0 \quad (4.34)$$

$$E_z = 0 \quad (4.35)$$

$$H_x = 0 \quad (4.36)$$

$$H_y = H_0 \sin\left(\frac{\pi}{W} z'\right) \quad (4.37)$$

$$H_z = 0 \quad (4.38)$$

Using equations (32) & (35)

$$E_{\phi} = +j \frac{k_0 h W E_0 e^{-j k_0 r}}{2 \pi r} \left\{ \sin \theta \frac{\sin(X)}{X} \frac{\sin(Y)}{Y} \right\} \quad (4.39)$$

Where,

$$X = \frac{k_0 h}{2} \sin \theta \cos \phi$$

$$Y = \frac{k_0 L_1}{2} \sin \theta \sin \phi$$

The array factor for the two elements in z-direction is,

$$(AF)_x = 2 \sin \left(\frac{k_0 W}{2} \cos \theta \right) \quad (4.40)$$

$$E_{\phi} = +j \frac{k_0 h W E_0 e^{-j k_0 r}}{\pi r} \left\{ \sin \theta \frac{\sin(X)}{X} \frac{\sin(Y)}{Y} \right\} \times \sin \left(\frac{k_0 W}{2} \cos \theta \right) \quad (4.41)$$

Putting the value of $\theta = 90^\circ$ in (4.41),

$$E_{\phi} = +j \frac{k_0 h W E_0 e^{-j k_0 r}}{\pi r} \left\{ \frac{\sin \left(\frac{k_0 h}{2} \cos \phi \right) \sin \left(\frac{k_0 L_1}{2} \sin \phi \right)}{\frac{k_0 h}{2} \cos \phi \frac{k_0 L_1}{2} \sin \phi} \right\} \quad (4.42)$$

Putting the value of $\phi = 0^\circ$ in (41)

$$E_{\phi} = +j \frac{k_0 h W E_0 e^{-j k_0 r}}{\pi r} \left\{ \sin \theta \frac{\sin \left(\frac{k_0 h}{2} \sin \theta \right) \sin \left(\frac{k_0 L_1}{2} \sin \theta \right)}{\frac{k_0 h}{2} \sin \theta \frac{k_0 L_1}{2} \sin \theta} \right\} \times \sin \left(\frac{k_0 W}{2} \cos \theta \right) \quad (4.43)$$

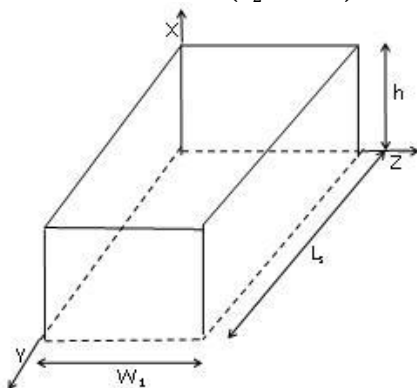


Figure 3. Second rectangle

The boundary conditions for 2nd rectangle shown in Figure3,

$$E_y(x' = 0, 0 \leq y' \leq L_s, 0 \leq z' \leq W_1) = E_y(x' = h, 0 \leq y' \leq L_s, 0 \leq z' \leq W_1) \quad (4.44)$$

$$H_y(0 \leq x' \leq h, 0 \leq y' \leq L_s, z' = 0) = H_y(0 \leq x' \leq h, 0 \leq y' \leq L_s, z' = W_1) \quad (4.45)$$

$$H_z(0 \leq x' \leq h, y' = 0, 0 \leq z' \leq W_1) = H_z(0 \leq x' \leq h, y' = L_s, 0 \leq z' \leq W_1) \quad (4.46)$$

From 2nd rectangle, $W_1 = 7.44$ mm, $L_1 = 14.445$ mm, $h = 1.6$ mm. So, $L_s > W_1 > h$ then the dominant mode is TM_{010}^x . The value of the k_x, k_y, k_z from (4.17), (4.18) & (4.19),

$$\text{Using } m = 0, n = 1, p = 0, \quad k_x = m\pi/h = 0 \quad (4.47)$$

$$k_y = n\pi/L_1 = \pi/L_s \quad (4.48)$$

$$k_z = p\pi/W_1 = 0 \quad (4.49)$$

Put the value of k_x, k_y, k_z in (4.24), (4.25), (4.26), (4.27), (4.28) & (4.29), we have the resultant fields,

$$E_x = E_0 \cos \left(\frac{\pi}{L_1} y' \right) \quad (4.50)$$

$$E_y = 0 \quad (4.51)$$

$$E_z = 0 \quad (4.52)$$

$$H_x = 0 \quad (4.53)$$

$$H_y = 0 \quad (4.54)$$

$$H_z = H_0 \sin \left(\frac{\pi}{L_1} y' \right) \quad (4.55)$$

Using (4.50) & (4.51)

$$E_{\phi} = +j \frac{k_0 h W_1 E_0 e^{-j k_0 r}}{2 \pi r} \left\{ \sin \theta \frac{\sin(X)}{X} \frac{\sin(Z)}{Z} \right\} \quad (4.56)$$

$$\text{Where, } X = \frac{k_0 h}{2} \sin \theta \cos \phi$$

$$Z = \frac{k_0 W_1}{2} \cos \theta$$

The array factor for the two elements in y-direction is,

$$(AF)_y = 2 \cos \left(\frac{k_0 h}{2} \sin \theta \sin \phi \right) \quad (4.57)$$

$$E_{\phi} = +j \frac{k_0 h W_1 E_0 e^{-j k_0 r}}{\pi r} \left\{ \sin \theta \frac{\sin(X)}{X} \frac{\sin(Y)}{Y} \right\} \times \cos \left(\frac{k_0 h}{2} \sin \theta \sin \phi \right) \quad (4.58)$$

Putting the value of $\theta = 90^\circ$ in (57)

$$E_{\theta} = +j \frac{k_0 h W_1 E_0 e^{-j k_0 r}}{\pi r} \left(\frac{\sin \left(\frac{k_0 h}{2} \cos \phi \right)}{\frac{k_0 h}{2} \cos \phi} \right) \times \cos \left(\frac{k_0 L_s}{2} \sin \phi \right) \quad (4.59)$$

Putting the value of $\phi = 0^\circ$ in (58)

$$E_{\theta} = +j \frac{k_0 h W_1 E_0 e^{-j k_0 r}}{\pi r} \left(\frac{\sin \left(\frac{k_0 h}{2} \sin \theta \right) \sin \left(\frac{k_0 W_1}{2} \cos \theta \right)}{\frac{k_0 h}{2} \sin \theta \frac{k_0 W_1}{2} \cos \theta} \right) \quad (4.60)$$

The final E-shape microstrip antenna equations by adding {(4.97) + (4.116)} and {(4.98) + (4.117)} is given below

$$E_{\theta} = +j \frac{k_0 h W E_0 e^{-j k_0 r}}{\pi r} \left(\frac{\sin \left(\frac{k_0 h}{2} \cos \phi \right) \sin \left(\frac{k_0 L_1}{2} \sin \phi \right)}{\frac{k_0 h}{2} \cos \phi \frac{k_0 L_1}{2} \sin \phi} \right) + j \frac{k_0 h W_1 E_0 e^{-j k_0 r}}{\pi r} \left(\frac{\sin \left(\frac{k_0 h}{2} \cos \phi \right)}{\frac{k_0 h}{2} \cos \phi} \right) \times \cos \left(\frac{k_0 L_s}{2} \sin \phi \right) \quad (4.61)$$

$$E_{\theta} = +j \frac{k_0 h W E_0 e^{-j k_0 r}}{\pi r} \left(\sin \theta \frac{\sin \left(\frac{k_0 h}{2} \sin \theta \right) \sin \left(\frac{k_0 L_1}{2} \sin \theta \right)}{\frac{k_0 h}{2} \sin \theta \frac{k_0 L_1}{2} \sin \theta} \right) \times \sin \left(\frac{k_0 W}{2} \cos \theta \right) + j \frac{k_0 h W_1 E_0 e^{-j k_0 r}}{\pi r} \left(\frac{\sin \left(\frac{k_0 h}{2} \sin \theta \right) \sin \left(\frac{k_0 W_1}{2} \cos \theta \right)}{\frac{k_0 h}{2} \sin \theta \frac{k_0 W_1}{2} \cos \theta} \right) \quad (4.62)$$

5. Result

The proposed antenna resonates at 2.46 GHz with return loss -13.5 dB and 2.886 GHz with return loss -14.7 dB. The -10 dB on simulation, antenna resonates at 2.082 GHz with return loss -22.77 dB, 2.514 GHz with return loss -20.54 dB and 2.874 GHz with return loss -19.27 dB.

In simulation and measurement the return loss has a negative which states that the losses are minimum during the transmission. The voltage standing wave ratio for the proposed antenna has a good value 1.207, it indicate that the level of mismatch is not so high. In future others different type of feed techniques can be used to calculate the overall performance of the antenna without missing the optimized parameters in the action.

As we can see that the all resonance frequency band lies between the frequencies band 2100MHz -2400MHz which is the band of 4G Systems. The obtained impedance bandwidth also covers the frequency band for 4G systems. So we can say that the proposed antenna works with 4G Systems.

a. Input impedance locus

The optimum feed position has been determined for good impedance matching shown in Figure 4, because the input impedance is controlled by the position of the probe to patch connection point. The used co-axial probe in designing of E-shape microstrip patch antenna made of Teflon with impedance 50 ohm.

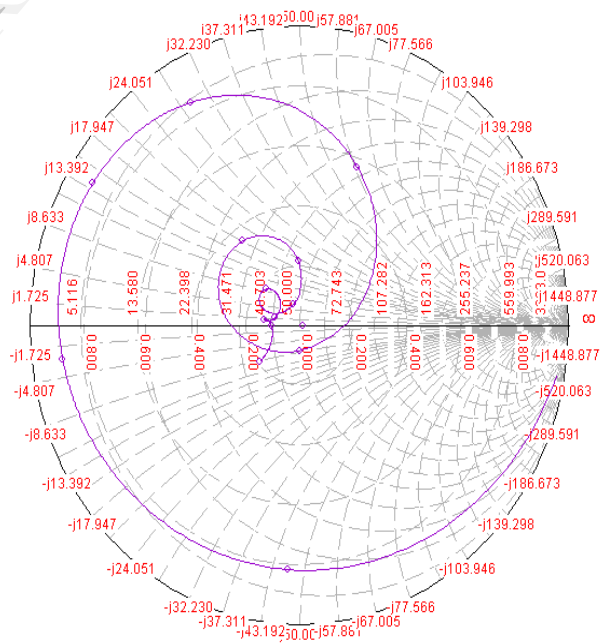


Figure 4. Input impedance loci

b. Return loss versus Frequency

The simulated plot between return loss and frequency is shown in Figure 5.

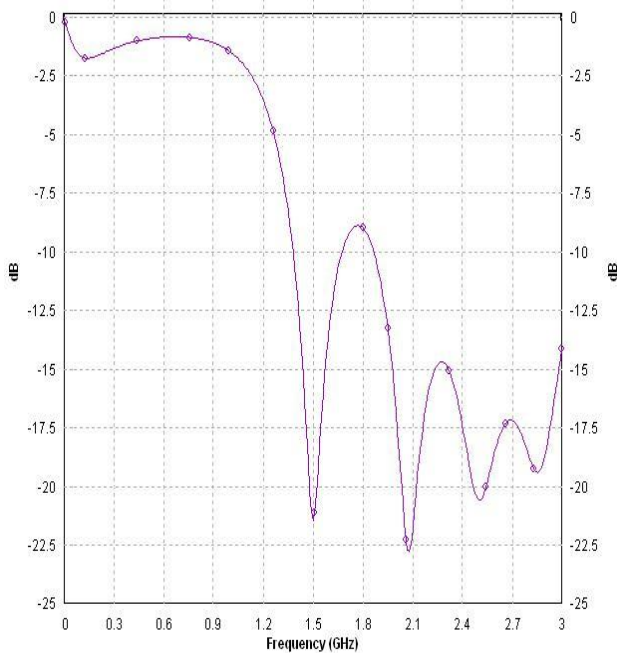


Figure 5. Return loss versus frequency plot

c. VSWR versus Frequency

The simulated plot between VSWR and frequency is shown in Figure 6.

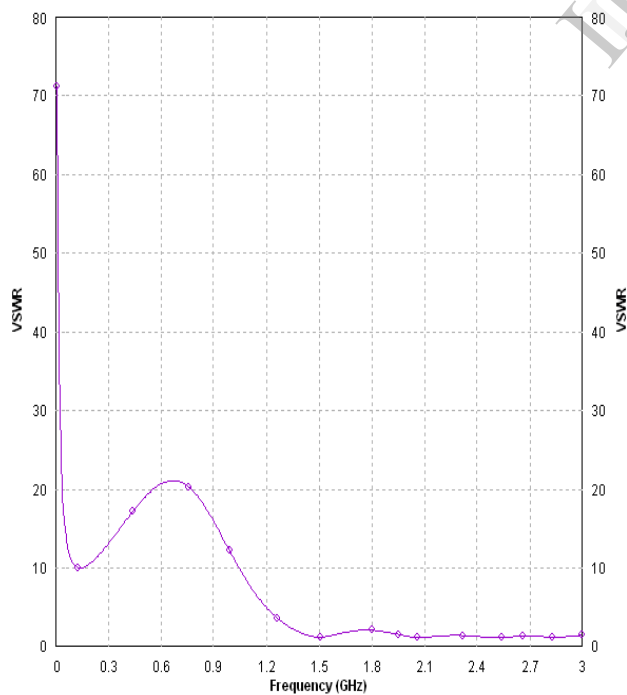


Figure 6. VSWR versus frequency plot

d. Radiation pattern

The simulated radiation pattern of proposed antenna is shown in Figure 7

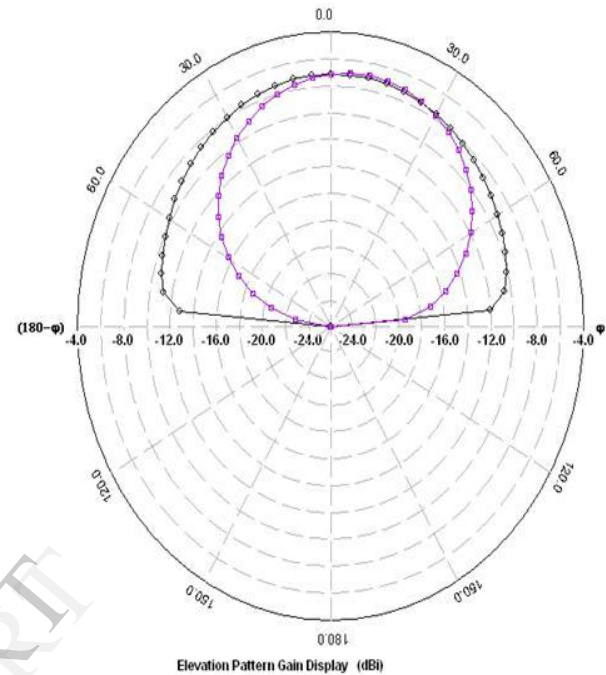


Figure 7. Radiation pattern

6. Conclusion and future prospectus

This paper presents the designing and analysis of the E-Shaped antenna is done using IE3D software and analysis is done by using Cavity Model method. In this paper, the prescribed antenna design is simulated over the value of the return loss and VSWR. From the simulation results, we can say that the E-shaped microstrip antenna gives the better results at operating frequency 3GHz. Without changing the permittivity and height of the substrate, the effect of various parameters of E-shaped patch antenna are studied. In simulation and measurement the return loss has a negative which states that the losses are minimum during the transmission. The voltage standing wave ratio for the proposed antenna has a good value 1.207, it indicate that the level of mismatch is not so high. In future others different type of feed techniques can be used to calculate the overall performance of the antenna without missing the optimized parameters in the action. In future others different type of feed techniques can be used to calculate the overall performance of the antenna without missing the optimized parameters in the action. The bandwidth can further enhanced by incorporated the different type of slots cutting in conventional rectangular microstrip antenna.

References

- [1] Constantine A. Balanis, "Antenna Theory, Analysis and Design", 2nd Edition, John Wiley & Sons, New York, 2005.
- [2] R. Garg, P. Bhartia, I. Bahl and A. Ittipiboon, "Microstrip Antenna Design Handbook", 1st Edition, Artech House, 2001.
- [3] Girish Kumar, K. P. Ray, "Broadband Microstrip Antennas", 1st Edition, Artech House, 2003.
- [4] Yi Huang, Kevin Boyle, "Antennas from Theory to Practice", 1st Edition, John Wiley & Sons, 2008.
- [5] Thomas A. Milligan, "Modern Antenna Design", 2nd Edition, John Wiley & Sons, 2005.
- [6] Zhi Ning Chen and Michael Y. W. Chia, "Broadband Planar Antennas Design and Applications", 1st Edition, John Wiley & Sons, 2006.
- [7] Richard C. Johnson, "Antenna Engineering Handbook", 3rd Edition, MGH, 1993.
- [8] Yuehe Ge, Karu P. Esselle and Trevor S. Bird, "E-shaped patch antennas for high-speed wireless networks", IEEE Transactions on Antennas and Propagation, vol. 52, no. 12, December 2004, pp. 3213-3219.
- [9] A. C. O. Pedra, G. Bulla, P. Serafini, C. R. Famandez, G. Monser and A. A. A. de salles, "Bandwidth and size optimization of a wide-band E-shape patch antenna", SBMO/IEEE MTT-S International Microwave & Optoelectronics Conference (IMOC2007), 2007, pp. 422-426.
- [10] Vijay K. Pandey and Babau R. Vishvakarma, "Analysis of an E-shaped patch Antenna", Microwave and Optical Technology Letters, vol. 49, no. 1, January 2007, pp. 4-7.
- [11] Tayeb A. Denidni, "Design of a wideband microstrip antenna for mobile handset applications", Technical Media Journal, LLC, High Frequency Electronics, February 2004, pp. 24-27.
- [12] Fan Yang, Xue-Xia Zhang, Xiaoning Ye, and Yahya Rahmat-Samii, "Wide-band E-shaped patch antennas for wireless communications", IEEE Transactions on Antennas and Propagation, vol. 49, no. 7, July 2001, pp. 1094-1100.
- [13] P. K. Singhal and Piyush Moghe, "Design of a single layer E-shaped microstrip patch antenna", Asia Pacific Microwave Conference (APMC2005 proceedings), Suzhou, China, Dec. 4-7, 2005.
- [14] Yuehe Ge, Karu P. Esselle and Trevor S. Bird, "Broadband E-shaped patch antennas for 5-6 GHz wireless computer networks", Electronics Letters, 2003, pp. 942-945.
- [15] B.-K. Ang and B.-K. Chung, "A wideband E-shaped microstrip patch antenna for 5-6 GHz wireless communications", Progress in Electromagnetics Research, PIER 75, 397-407, 2007.
- [16] A. A. Deshmukh and G. Kumar, "Compact broadband E-shaped microstrip antennas", Electronics Letters, 1st Sep. 2005, vol. 41, no. 18.
- [17] Amit A. Deshmukh and Girish Kumar, "Compact E and S-shaped microstrip antennas", Electronics Letters, 2005, pp. 389-392.
- [18] A. M. El-Teger and A. M. Abdin, "Design of multi-band dual-polarized two-port E-shape microstrip antenna", Progress in Electromagnetic Research Symposium, Beijing, China, March 23-27, 2009.
- [19] IE3D 12.0, User's Manual, Zeland Software Inc., Fremont, CA 94538, Oct. 2007.